Available online at www.sciencedirect.com
SCIENCE DIRECT®
Biochemical Pharmacology 68 (2004) 2009–2017
Biochemical Pharmacology
www.elsevier.com/locate/biochempharm

Inhibition of insulin-like growth factor I receptor tyrosine kinase by ethanol

Raphael Rubin[a,*], Rob Harrison[b], Xian-Feng Chen[b], Joseph Corzitotto[a], Jan B. Hoek[a], Hazem Hallak[a]

[a]*Department of Pathology, Anatomy and Cell Biology, Jefferson Medical College, 226 Alumni Hall, Philadelphia, PA 19107, USA*
[b]*Departments of Computer Science and Biology, Georgia State University, Atlanta, GA 30303, USA*

Received 3 May 2004; accepted 28 June 2004

Abstract

Ethanol inhibits insulin and insulin-like growth factor-I (IGF-I) signaling in a variety of cell types leading to reduced mitogenesis and impaired survival. This effect is associated with inhibition of insulin receptor (IR) and insulin-like growth factor-I receptor (IGF-IR) autophosphorylation, which implicates these receptors as direct targets for ethanol. It was demonstrated previously that ethanol inhibits the autophosphorylation and kinase activity of the purified cytoplasmic tyrosine kinase domain of the IR. We performed computer modeling of the ethanol interaction with the IR and IGF-IR kinases (IRK and IGF-IRK). The analysis predicted binding of alcohols within the hydrophobic pocket of the kinase activation cleft, with stabilization at specific polar residues. Using IGF-IRK purified from baculovirus-infected insect cells, ethanol inhibited peptide substrate phosphorylation by non-phosphorylated IGF-IRK, but had no effect on the autophosphorylated enzyme. In common with the IRK, ethanol inhibited IGF-IRK autophosphorylation. In cerebellar granule neurons, ethanol inhibited autophosphorylation of the apo-IGF-IR, but did not reverse IGF-IR phosphorylation after IGF-I stimulation. In summary, the findings demonstrate direct inhibition of IGF-IR tyrosine kinase by ethanol. The data are consistent with a model wherein ethanol prevents the initial phase of IRK and IGF-IRK activation, by inhibiting the engagement of the kinase activation loop.

Keywords: Ethanol; Insulin receptor; Insulin-like growth factor-I receptor; Tyrosine kinase; Cerebellar granule neurons

The interaction of ethanol with intracellular signal transduction pathways has been linked to disturbances in cell proliferation and survival [1]. Such perturbations may play a role in the pathogenesis of certain disorders of tissue and organ function associated with acute and chronic alcohol exposures, including neuronal degeneration, cirrhosis, myopathy, and cardiomyopathy. Maternal alcohol consumption during gestation causes profound disorders of fetal brain development (fetal alcohol syndrome) [2].

IGF-I and insulin induce proliferation and survival in most cell types [3,4]. Pharmacologically relevant concentrations of ethanol inhibit intracellular signaling responses to IGF-I and insulin, leading to impaired cell growth and survival [5–12]. As a common feature, ethanol inhibits the autophosphorylation of the IGF-I receptor (IGF-IR) and the insulin receptor (IR) [5,6,11–14], which is the initial step in receptor activation following ligand binding. Inhibition of tyrosine autophosphorylation of the platelet-derived growth factor-bb receptor [15] and the FGF receptor [16] have also been observed in certain cell types. By contrast, the EGF receptor and other members of the PDGF receptor family are largely insensitive to these acute actions of ethanol.

The IR and IGF-IR are closely homologous [17], and the repertoire of signaling molecules that are activated by their ligands are remarkably similar [3]. The receptors are composed of α2–β2 heterodimers, the individual chains linked by α–α and α–β disulfide bridges. The extracellular ligand binding domain is constituted on the α chain, and the tyrosine kinase domain is on the intracellular β domain.

Abbreviations: IGF-I, insulin-like growth factor-I; IGF-IR, IGF-I receptor; IGF-IRK, IGF-IR kinase; IR, insulin receptor; IRK, IR kinase; FGF, fibroblast growth factor; IRS-1, insulin-related substrate-1; EGF, epidermal growth factor; PDGF, platelet-derived growth factor.

* Corresponding author. Tel.: +1 215 503 4517; fax: +1 215 955 8703.
E-mail address: raphael.rubin@jefferson.edu (R. Rubin).

0006-2952/$ – see front matter © 2004 Elsevier Inc. All rights reserved.
doi:10.1016/j.bcp.2004.06.032

Sequence homology is greatest within the tyrosine kinase domain (>80%), and diverges within the carboxyterminal domains, which may account for some of the different functions of the IR and IGF-IR. Notably, IGF-I and insulin principally exert mitogenic and metabolic actions, respectively [18]. Upon ligand binding, the receptors undergo rapid autophosphorylation within the tyrosine kinase domain (Y1131, Y1135 and Y1136 in the IGF-IR and Y1158, Y1162 and Y1163 in the IR). Other tyrosines that are targets for phosphorylation are found within the juxtamembrane and carboxyterminus domains.

The mechanism by which ethanol inhibits the IGF-IR and IR has only been partially characterized. Ethanol inhibits the tyrosine autophosphorylation of IGF-IR within immunoprecipitants [13]. This result suggests that that ethanol directly interacts with the IGF-IR, although a role for ethanol interaction with other proteins contained within the IGF-IR immunoprecipitant complex could not be excluded. To address this issue, we tested the effect of ethanol on the activity of the minimally-defined IR kinase (IRK) [19]. Ethanol inhibited the tyrosine kinase activity of soluble GST-IR, both in terms of the phosphorylation of peptide substrate and autophosphorylation. Kinetic analysis of peptide phosphorylation indicated a non-competitive inhibition by ethanol, with a reduction in the V_{max} of 21% at 150 mM ethanol. These data suggested that the inhibitory effect of ethanol on this class of receptors is localized to the cytoplasmic kinase domain.

The crystal structures of the IR and the IGF-IR kinases (IRK and IGF-IRK) have been solved [20–24], which has provided insights into their activation dynamics. The IR and IGF-IR cytoplasmic kinase domains are highly homologous with 84% overall identity, and 100% identity within the ATP binding cleft [17]. Indeed, by X-ray crystallography, the root-mean square deviation for the Cα atoms of the IR and IGF-IR is 2.5 Å [21]. The kinases are comprised of an N-terminal lobe comprising a five beta-stranded β sheet and one α helix, and a larger carboxyterminal lobe that is mainly α-helical. The activation loop (A-loop) is located in the larger carboxyterminal lobe. ATP binds within the cleft between the two lobes, and tyrosine-containing substrates bind to the carboxyterminal lobe.

The conversion of inactive IRK/IGF-IRK to their active forms involves conformational changes in the protein with a swing-out of the A-loop, thereby allowing access of substrates to the catalytic site [25]. A key regulatory feature of both the IRK and IGF-IRK is that tyrosines within the A-loop (Y1162 for IR and Y1131 for IGF-IR) are bound within the active site, hydrogen-bonded to conserved polar residues within the catalytic loop [20,22]. In the unphosphorylated (0P) state, internal stabilizations prevent phosphorylation of substrates ('gate-closed' configuration) resulting in an autoinhibited state. However, autoinhibition is sufficiently weak to allow for a transient 'gate-open' configuration thereby allowing for transphosphorylation after ligand binding. Thus, autophosphorylation of the IR and the IGF-IR kinases increases their catalytic efficiencies. Based upon these considerations, it was demonstrated that intermolecular transphosphorylation is required to relieve this steric constraint [21,23,26].

In the current study, we generated a model for the interaction of ethanol with the IR and IGF-IR kinases, which predicts binding of ethanol and higher chain n-alkanols within the kinase activation clefts. To validate this model, we tested the effect of ethanol on the IGF-IRK tyrosine kinase domain. The data demonstrate inhibitory action of ethanol on the IGF-IRK, and are consistent with a mechanism whereby ethanol interferes with the initial phase of kinase activation involving the mobilization of the conserved kinase activation loop.

1. Materials and methods

1.1. Materials

Synthetic IRS-1 peptide KKEEEEYMMMMG was synthesized by Biosource (Camarillo, CA). [γ-^{32}P]ATP was from DuPont NEN (Boston, MA). Human recombinant IGF-I was from Calbiochem (San Diego, CA). Anti-IGF-IR β-subunit rabbit polyclonal antibodies and anti-phosphotyrosine (PY99) mouse monoclonal antibodies were obtained from Santa Cruz Biotechnology (Santa Cruz, CA). Anti-MAP kinase antibodies, anti-phosphotyrosine and phosphothreonine MAP kinase (E10) antibodies, horseradish peroxidase-conjugated goat anti-rabbit IgG, horse anti-mouse IgG antibodies and signal-enhanced chemiluminescence reagents were obtained from New England Biolabs (Beverly, MA). All other chemicals and biochemicals were of the highest purity commercially available.

1.2. Expression and purification of IGF-IR kinases

The BAC-To-BAC Baculovirus expression system (Invitrogen; Carlsbad, CA) was used to express the IGF-IR cytoplasmic kinase domain fused to a 6-His tag. cDNA corresponding to IGF-IRK residues 956–1256 subcloned into pFB vector was obtained from Dr. Todd Miller, Stoneybrook, NY. IGF-IR was released with *Eco*RI and *Hin*dIII, and ligated into pFastBac HTc plasmids. Generation of recombinant bacmid, infection of *Spodoptera frugiperda* (Sf9) cells, and purification over NiNTA resin columns were performed according to the manufacturers specifications. Protein were concentrated using Microcon YM-10 centrifugal filter devise (Millipore; Bellerica, MA), resuspended in 50 mM Hepes, pH 7.5, and stored at 4 °C. Protein concentration was determined using the Bradford method (Bio-Rad; Hercules, CA).

1.3. Peptide phosphorylation

Phosphorylation of IRS-1 peptide was measured using a filter binding assay as described previously [19]. Kinase buffer contained 50 mM HEPES, pH 7.5, 10 mM $MgCl_2$, 2 mM $MnCl_2$, 1 mM peptide, 0.1 mg/ml bovine serum albumin, 50 μM ATP and 70 μCi/ml [γ-^{32}P]ATP. Phosphorylations were performed for 10 min at room temperature. Reactions were started by the addition of 50 nM enzyme. Peptide phosphorylations were linear up to 15 min in all cases. Alcohols were added 15 min prior to the initiation of the reaction. Reactions were terminated by the addition of 10% TCA, and then applied onto 2.1 cm diameter P81 phosphocellulose paper (Whatman; Hillsboro, OR). Filters were washed extensively with ice-cold 0.5% TCA, once with acetone, and dried. Incorporation of ^{32}P into the peptide substrate was quantitated by liquid scintillation counting.

1.4. Kinase autophosphorylation

IGF-IR autophosphorylations were assayed in kinase buffer containing 0.4 mM [γ^{32}P]ATP. Ethanol was added 15 min prior to the addition of ATP. At the indicated times, the reactions were stopped with Laemmli buffer, and the phosphorylated proteins were visualized by SDS-PAGE and autoradiography. The Coomassie blue stained proteins were cut out, and the radioactivity determined by liquid scintillation counting. For separation of unphosphorylated from phosphorylated kinase, reactions were quenched in 50 mM EDTA and separated by electrophoresis on 10% non-denaturing Tris–HCl native agarose gels (Bio-Rad).

1.5. Preparation of cerebellar granule neurons

Rat cerebellar granule neurons were prepared from 7-day-old rat pups as reported previously [7,27]. Briefly, cerebella were cross-chopped, and then treated at 37 °C with 0.025% trypsin-EDTA (including 0.01% DNase I) for 15 min. Cells were triturated and plated at a density of 1×10^6/cm^2 on poly-D-lysine-coated plates in basal medium eagle (BME) containing 10% fetal bovine serum, 25 mM KCl, 100 units/ml penicillin, 100 μg/ml streptomycin, and 0.25 μg/ml amphotericin B. 10 μM cytosine arabinoside was added after 24 h to inhibit non-neuronal replication. Cerebellar neurons were used after 7 days in vitro. Cells were washed 3 times and incubated in BME without serum for 6 h prior to addition of IGF-I.

1.6. Immunoprecipitations and Western blot analysis

Cerebellar granule neurons were lysed in ice-cold Triton lysis buffer (50 mM HEPES, pH 7.5, 150 mM NaCl, 1.5 mM $MgCl_2$, 1 mM EGTA, 0.5 mM EDTA, 10% glycerol, 1% Triton X-100, 100 mM NaF, 2 mM Na_3VO_4, 10 mM sodium PP_I, 10 mM phenylmethylsulfonylfluoride, 500 μM AEBSF, 150 nM aprotinin, 1 μM E-64, and 1 μM leupeptin). The lysates were centrifuged at 14,000 × *g* for 10 min at 4 °C, and the supernatants collected. For immunoprecipitations, supernatants were diluted with 1 volume of HNTG (20 mM HEPES, pH 7.5, 150 mM NaCl, 0.1% Triton X-100, 10 mM of NaF and 2 mM Na_3VO_4). Equal amounts of protein (250 μg) from each sample were immunoprecipitated using 0.4 μg/ml of antibody to IGF-IR, and captured using protein A agarose beads. Immunoprecipitates or cell lysates (30 μg protein) were electrophoresed in 11% denaturing polyacrylamide gels (SDS-PAGE), transferred to Immobilon-P membranes, and visualized by Western blotting. For Western blot analysis the membranes were blocked with 3% BSA and probed with antibodies (1:1000), followed by secondary horseradish peroxidase-conjugated goat anti-rabbit IgG or horse anti-mouse IgG antibodies. Membranes were visualized by enhanced chemiluminescence (Amersham Pharmacia Biotech).

2. Results

2.1. Modeling of alcohol interaction with IRK and IGF-IRK

The binding of alcohols and water with the IRK and IGF-IR were predicted using the program Dynama [28,29]. The potential is exactly the same as is used in a molecular mechanics program like AMMP [30,31] and corresponds to a strategy using a Monte-Carlo algorithm with importance sampling to evaluate the partition function for the pair of molecules. This program uses an algorithm (O(N lgN)) and Fourier transform to rapidly evaluate a molecular mechanics representation of the interaction energy between two molecules as a function of their relative orientations. The molecular mechanics representation includes terms that represent Van der Waals interactions, charge–charge interactions and reproduces effects of hydrogen bonds and salt bridges as represented in the molecular potential. The protein molecule is kept fixed, and the conformational space of the small molecule probe is explored by running short lengths of molecular dynamics between rotational sampling. It produces two outputs: (1) the locations and relative orientations of energy minima, and (2) a three-dimensional map of the energy. Both of these outputs can be used to visualize the results.

Fig. 1, panel A illustrates structural features of the unphosphorylated IRK. Coordinates were obtained from the apo-form of the IRK without ATP analogue. A hydrophobic crevice is formed by apposition of the N- and C-terminal lobes (hydrophobic amino acids in blue). The activation loop (residues 1149–1179) is highlighted (yellow). Energy minima for the interaction of individual octanol molecules with the apo-IRK were generated and visualized. Calculations performed on the alcohols were

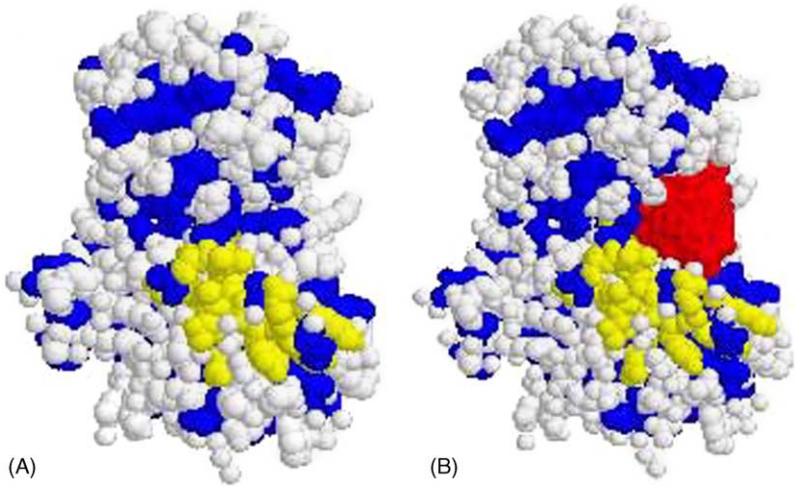

Fig. 1. Dynama modeling of octanol binding to IRK. (Panel A) Spacefill representation of apo-IRK. Blue: Hydrophobic residues; Yellow: Activation loop (aa 1149–1179). (Panel B) Dynama modeling for octanol (red) interaction with IRK.

normalized by dividing with the partition function from the water calculation as described previously [29]. Dynama modeling (Fig. 1, panel B) reveals binding of octanol (red) within the hydrophobic activation cleft.

The interaction of alcohols with hydrophobic domains in diverse proteins is stabilized by interaction of the hydroxyl group with polar moieties via hydrogen bonding [32]. Dynama modeling of the interaction of octanol and hexanol (not shown) with the apo-IRK predicted hydroxyl group hydrogen bonding for Lys1030, Glu1047, and Arg1131 (in the catalytic loop), and Ser1006 (in the nucleotide binding loop). Arg 1136 and Arg 1155 also participate in forming the binding pocket for alcohols.

Dynama modeling of the interaction of ethanol with the apo-IRK and the apo-IGF-IRK was performed (Fig. 2). As in the case of octanol, there was binding of ethanol (blue) within the activation clefts of both kinases. When the calculations were applied to models of the activated kinase in the closed conformation, the locations and values of the energy minima shift. Importantly, the alcohol-binding pocket is lost upon closure of the lobes with activation as manifest by a loss of the minima (not shown).

The binding of alcohols within the hydrophobic pocket of the activation cleft and its stabilization by polar residues suggests a mechanism by which alcohols could inhibit the enzyme. The reaction path for kinase activation proceeds

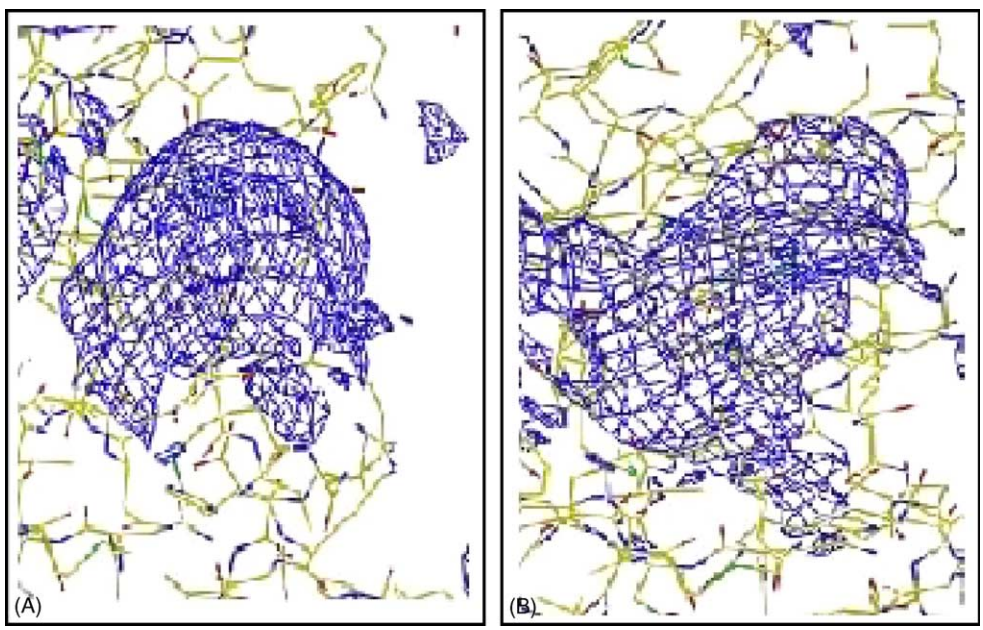

Fig. 2. Dynama modeling of ethanol (blue) binding within activation clefts of IRK (panel A) and IGF-IRK (panel B).

from the apo-form over a transition barrier into the active form. It is difficult to estimate the height of the reaction barrier by calculation, but thermodynamic considerations can be applied to understanding the relative energy levels of the apo- and active forms of the kinase. If the energy level of the apo-form of the enzyme is lowered by alcohol binding to a greater extent than its effect on active conformation, then the alcohol acts like an inhibitor because it shifts the equilibrium towards the apo-form. The results of the calculations on alcohols and the apo-form of the kinase suggest that the enzyme strongly binds alcohols in the apo-form, and the alcohol binding pocket is lost in the active form. In effect, alcohol binding within the activation cleft might shift the A-loop equilibrium towards the inactive 'gate-closed' configuration. Increased alcohol hydrophobicity with longer chain lengths would be expected to further stabilize the inactive enzyme. Two thermodynamic and energetic effects would cause the longer chain alcohols to be better inhibitors. First, there would be an increased interaction energy between the enzyme and the alcohol due to the larger number of atoms that can interact with Van der Waals and other non-bonded interactions. Second, longer chain alcohols are less soluble in water than short chain alcohols, and therefore would be expected to show a much higher hydrophobic effect leading to a higher binding energy.

Taken together, these considerations allow us to predict the following: (1) kinase activity of unphosphorylated kinase would be inhibited by ethanol, whereas autophosphorylated ('gate-open') kinase (which is stabilized by phosphotyrosine and non-phosphotyrosine interactions) would be less sensitive to ethanol; and (2) the potency of inhibition by alcohols will vary directly with hydrophobicity.

2.2. Purification of IGF-IRK

IGF-IRK was purified from recombinant baculovirus-infected Sf9 insect cells. Fig. 3 illustrates the time course of IGF-IRK autophosphorylation assayed by ^{32}P-phosphotransfer. Following a brief lag phase, there was linear radiolabel incorporation for up to 15 min. The calculated molar ratio of ^{32}P incorporation did not exceed 1 mol phosphate/mol enzyme, thereby suggesting incomplete phosphorylation of the A-loop. Incomplete

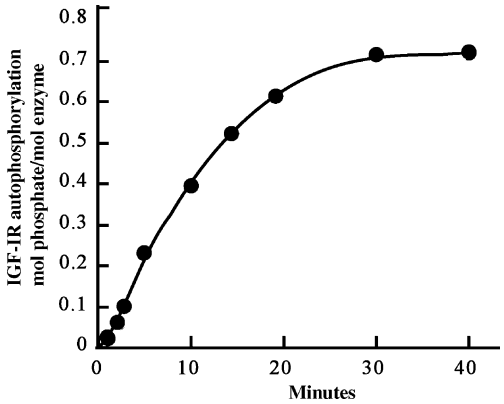

Fig. 3. IGF-IRK autophosphorylation. (^{32}P)Autophosphorylation of IGF-IRK (1 μM) was performed as described under Material and Methods. Samples were taken at the indicated times for SDS-PAGE and the kinase was visualized by autoradiography.

phosphorylation likely represents dephosphorylation activity [21].

To measure the conversion of unphosphorylated IGF-IRK (0P) to mono-, bis-, and tris-phosphorylated forms (1P, 2P, and 3P), the differently phosphorylated forms were resolved by non-denaturing agarose gel electrophoresis (Fig. 4). 1P and 2P forms were evident at 5 min and increased by 20 min, concomitant with a marked decline in the 0P form. A mixture of 1P, 2P, and 3P persisted at 20 min, once again reflecting incomplete A-loop phosphorylation.

2.3. Ethanol inhibits kinase activity of apo-IGF-IRK

Based upon the model presented above, we tested the effect of IGF-IRK phosphorylation on its sensitivity to ethanol. Kinase activity was assayed using the IRS-1 peptide KKEEEEYMMMMG [33]. Fig. 5 demonstrates that there was a pronounced increase in kinase activity after autophosphorylation Autophosphorylation of the 0P enzyme does not occur in the presence of peptide and the low ATP concentrations used in the phosphorylation assay [23]. Ethanol (100 mM), butanol (2 mM), hexanol (1 mM), and octanol (0.1 mM) inhibited the activity of 0P IGF-IR by up to 25%, but had no effect on peptide phosphorylation by the autophosphorylated enzyme, with the minor exception of octanol. Autophosphorylation of

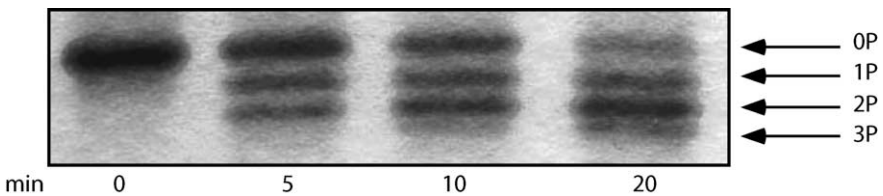

Fig. 4. IGF-IRK autophosphorylation: native gel electrophoresis. IGF-IRK (5 μM) was incubated with 100 μM ATP. At the indicated times, samples were quenched in 50 mM EDTA and 0P, 1P, 2P, and 3P forms of IGF-IRK separated on non-denaturing Tris–HCl native agarose gels and visualized by Coomassie blue staining.

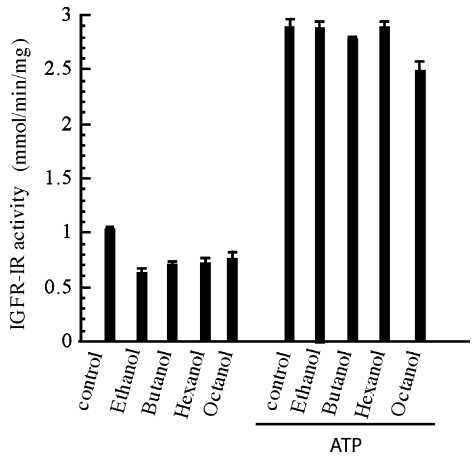

Fig. 5. N-alkanols inhibit non-phosphorylated form of IGF-IRK. IGF-IRK (25 μM) was incubated with ATP (0.75 mM) for 30 min. Aliquots of either 0P or phosphorylated kinase (50 nM) were then used for assay of IRS-1 peptide phosphorylation assays in the presence or absence of the indicated alcohols (100 mM ethanol, 2 mM butanol, 1 mM hexanol, 0.1 mM octanol). The data represent the mean ± S.D. of triplicate determinations from a representative experiment.

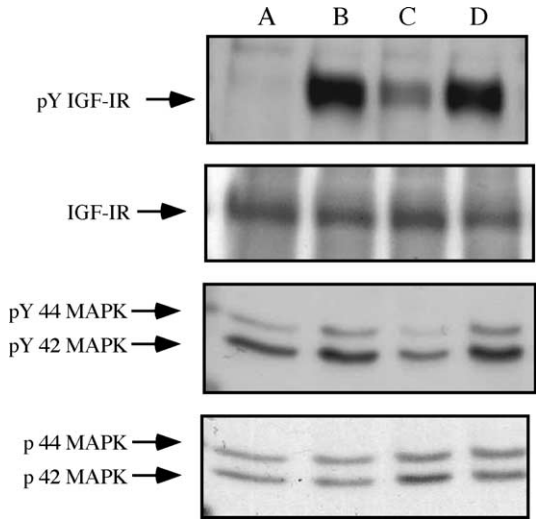

Fig. 7. Ethanol inhibits IGF-IR activation in cerebellar granule neurons. Cerebellar granule neurons were stimulated with IGF-I (20 ng/ml) for 10 min. Lane A: Control without IGF-I; Lane B: IGF-I; Lane C: IGF-I plus ethanol (100 mM) added before IGF-I; Lane D: Ethanol added 5 min after IGF-I. IGF-IR was immunoprecipitated and tyrosine phosphorylation and total content were measured by Western blotting. Lysates were used for visualization of phospho-MAPK and total MAPK.

GST-IRK induced a 300% increase in kinase activity, and the kinase activity of the phosphorylated IRK was not inhibited by 100 mM ethanol (data not shown). Thus, similar to the IGF-IRK, ethanol inhibited the activity of the 0P form of IRK [19].

Ethanol inhibited the autophosphorylation of the IGF-IR kinase (Fig. 6). 50 mM ethanol inhibited IGF-IR autophosphorylation by 8%, and near-maximal inhibition (20%) was observed at 100 mM ethanol, which is similar in magnitude to the effect of ethanol on the IRK [19].

2.4. Inhibition of IGF-IR autophosphorylation in intact cells

The data presented above indicates that the initial phase of IGF-IR autophosphorylation is inhibited by ethanol, whereas kinase activity of the phosphorylated IGF-IR is insensitive. To test whether this occurs in intact cells, we studied the effect of ethanol on IGF-IR tyrosine autophosphorylation in cerebellar granule neurons (Fig. 7). IGF-IR tyrosine phosphorylation was undetectable after serum starvation. IGF-I induced phosphorylation of the IGF-IR and MAPK, which were markedly inhibited by ethanol. By contrast, ethanol had no effect on the phosphorylation of IGF-IR or MAPK when added 5 min after IGF-I.

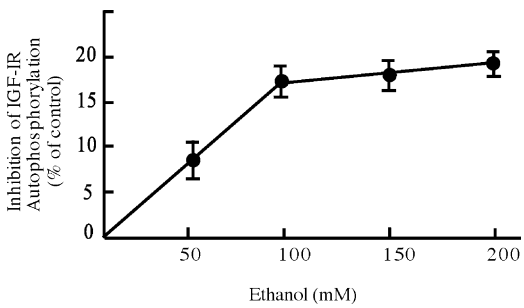

Fig. 6. Concentration dependence of ethanol for inhibition of IGF-IRK autophosphorylation. IGF-IRK (1 μM) was (^{32}P)autophosphorylated as described in Fig. 7 in the absence or presence of the indicated concentrations of ethanol. The data represent the means ± S.D. of triplicate determinations from a representative experiment.

3. Discussion

Myer [34] originally observed that the anesthetic properties of alcohols and anesthetics correlate directly with their hydrophobic lipid partitioning. The bulk interaction of ethanol with plasma membranes was later conjectured to account for cellular dysfunction, perhaps owing to perturbation of protein function that follows membrane disordering by ethanol. It is now clear that ethanol can also alter the functional properties of an array of proteins following direct hydrophobic interactions at specific sites [32]. It has been demonstrated for several proteins that ethanol accumulates within specific hydrophobic pockets, and there is interaction of the hydroxyl group with polar moieties via hydrogen bonding. N-alkanols can affect the function of purified protein function in vitro. Seminal studies by Franks and co-workers initially demonstrated inhibition of purified firefly luciferase [35,36]. Ethanol interacts with protein kinase C [37], phospholipase A_2 [38], and several ion channels [39,40].

In the current study, we have demonstrated inhibitory action of ethanol on IGF-IRK purified from baculovirus-infected Sf9 cells. Ethanol inhibits the non-phosphorylated (0P) enzyme, but is ineffective against autophosphorylated

kinase wherein exists the 'gate-open' configuration of the A-loop. The data are consistent with an ethanol-induced shift in the A-loop equilibrium in the 0P form to the 'gate-closed' position, thereby reducing transphosphorylation, which is key to the initial phase of autophosphorylation. This view is supported by the finding in intact neurons that ethanol inhibited IGF-IR autophosphorylation and activation of MAPK, but did not reverse these parameters after IGF-I activation. This further suggests that the effects of ethanol are not mediated by activation of tyrosine phosphatases.

This interpretation of these experimental findings is supported by structural modeling, which predicts accumulation of ethanol within the hydrophobic environment of the IRK and IGF-IRK activation clefts, with stabilization by hydrophilic interactions at polar amino acid residues. As for other proteins studied [32], it is unlikely that such alcohol accumulation within the activation cleft alters the structure of the proteins. Rather, for enzymes in particular, alcohols likely stabilize certain conformations of the catalytic activation cycle. Such stabilization might translate to higher substrate K_m's, as was demonstrated previously for the IRK [19]. In the case of the IRK and IGF-IRK, ethanol might inhibit activation loop swing out, or, alternatively, interfere with closure of the hydrophobic adenine binding loop.

Several additional lines of evidence favor direct ethanol interactions with proteins as opposed to bulk membrane disordering: (1) The binding of alcohols to proteins is saturable, indicating weak and unconstrained interactions [32]. Saturability of the inhibition of IGF-IRK by ethanol was observed in this study, and previously for the IRK [19]. (2) Binding and functional effects of alcohols frequently exhibit a 'cut-off' at longer chain lengths, indicative of specific binding sites within hydrophobic pockets [39]. We did not observe a cut-off of alcohol inhibition of IRK through dodecanol (R. Rubin, unpublished data). However, by modeling, there do not appear to be any spatial constraints for longer-chain n-alkanols within the hydrophobic pocket considered for the IRK and IGF-IRK. (3) Crystallographic data have identified common motifs within ethanol binding sites [32]. Interaction between a pair of alpha helixes appears important. Such sites are found within the hydrophobic adenine binding site of the IGF-IRK and IRK [25]. (4) In addition to hydrophobic interactions, there is an important role for hydrogen bonding in that alkanols displace water, and act as weak H^+-donors [41,42]. Hydrogen bonding to polar side chains and peptide carbonyl groups occurs, and may affect both interchain and intrachain interactions. (5) A series of studies of alkanol effects on ion channels (e.g. GABA, glycine, acetylcholine, K^+), have identified key sites that confer functional sensitivity to n-alkanols. In general, generation of chimeras between sensitive and insensitive proteins, and mutagenesis of key amino acids have confirmed the notion that alcohol binding within hydrophobic pockets is important for modulation of ion channel activity [43–47]. For example, in a study of GABA receptor activation by ethanol [48] the efficacy of different amino acid mutations correlated directly with the alteration of the volume of the hydrophobic pocket.

While the basal phosphorylation status of the IGF-IR appears to be important for their sensitivity to ethanol, myriad other intracellular and extra-cellular factors undoubtedly influence the global effects of ethanol on insulin or IGF-I signaling. Such factors include α subunit interactions, membrane sub-domain distribution, receptor complex internalization, receptor transphosphorylation, phosphatase activity, and a host of intracellular binding proteins. Indeed, the sensitivity of a several ion channels and other membrane-associated proteins to ethanol is influenced by phosphorylations and other uncharacterized modifications [49]. In the case of IGF-I signaling, we have characterized subclones of 3T3 cells with overexpression of the IGF-IR that are resistant to ethanol, despite similar expression and basal phosphorylation status [10]. Additionally, in a series of neuronal cell types, there was diversity in the sensitivity of IGF-IR autophosphorylation to ethanol, despite ubiquitous inhibition of MAPK activation in the presence of IGF-I. Whether the insensitivity of the IGF-IR to ethanol under certain conditions is the result of covalent modification of the receptor, or, alternatively, reflects a role for additional proteins, is unknown.

The current findings present a locus within the IGF-IRK that might account for inhibitory actions of ethanol on IGF-I and insulin signaling. We also recently demonstrated that ethanol inhibits FGF-dependent vascular smooth muscle proliferation and autophosphorylation of the FGF-2 receptor [16], which bears close structural homology with the IRK and IGF-IRK within the tyrosine kinase domain [50]. Given the conserved structure of tyrosine kinase domains in general [25], we suggest that the current findings are relevant to other kinases that exhibit sensitivity to ethanol. Interestingly, we have been unable to demonstrate inhibition of epidermal growth factor receptor autophosphorylation by ethanol in several cell types. However, epidermal growth factor receptor kinase activity is one of the few tyrosine kinase receptors that does not require phosphorylation of the activation loop for maximal activity [51].

Xu et al. [52] recently demonstrated that IRβ tyrosine phosphorylation is reduced in the cerebella of rat pups in an experimental rat model of chronic gestational ethanol feeding, and reductions in the activation of signaling mediators downstream of the IR, including IRS-1, PI 3-kinase, and Akt kinase, and with impaired neuronal survival ex vivo. Whether the acute effects of ethanol on receptor tyrosine kinase activity relates to long-term changes in signaling potential remains to be determined.

Molecular mechanics-based modeling [31] is potentially a powerful mechanism for understanding the relation

between molecular structure and molecular properties. The program used in this work, Dynama, implements this approach via a Fourier transform to speed up the calculations and search a wide range of relative orientations and configurations between two molecules. Example calculations where this potential and this approach have successfully explained or correlated between theory and experiment include a wide range of enzyme systems, including trypsin, HIV protease, RSV protease, and glucokinase [31,53,54]. In these examples correlations between experimental and theoretical results have been as high as 90%, and even when lower, as is more typically the case, are usually statistically significant by a strong margin. One important feature of a program like Dynama is that it generates a map of the distribution of small molecules. This density, or more specifically the difference between the best solutions and the average solutions, results in a qualitative assessment of the range of bound configurations. It is also possible to perform a calculation similar to a cluster integral and to use this calculation to partially normalize the results to treat the effects of solvation.

The use of this approach for understanding the effects of alcohols on the IRK and IGF-IRK is particularly interesting because there appears to be a specific binding effect rather than a general unfolding or denaturing of the protein. Unlike other examples where we have used these approaches [28], the alcohols appear to bind in the active site region of the protein, but do not form a highly ordered complex. Calculations of molecular distributions, rather than of specific complexes, may be an important step to understanding the effects of relatively unstructured binding of alcohols to proteins. Ultimately, the specific interactions of ethanol or higher chain n-alkanols with the IRK or IGF-IRK awaits direct analysis by crystallographic methods.

Acknowledgments

This work was supported by National Institutes of Health Grants RO1 AA0976 (to R.R.).

References

[1] Luo J, Miller MW. Growth factor-mediated neural proliferation: target of ethanol toxicity. Brain Res Brain Res Rev 1998;27:157–67.
[2] Hannigan JH, Armant DR. Alcohol in pregnancy and neonatal outcome. Semin Neonatol 2000;5:243–54.
[3] Rubin R, Baserga R. Insulin-like growth factor-I receptor. Its role in cell proliferation, apoptosis, and tumorigenicity. Lab Invest 1995;73:311–31.
[4] LeRoith D, Werner H, Beitner-Johnson D, Roberts Jr CT. Molecular and cellular aspects of the insulin-like growth factor I receptor. Endocr Rev 1995;16:143–63.
[5] Resnicoff M, Cui S, Coppola D, Hoek JB, Rubin R. Ethanol-induced inhibition of cell proliferation is modulated by insulin-like growth factor-I receptor levels. Alcohol Clin Exp Res 1996;20:961–6.
[6] Banerjee K, Mohr L, Wands JR, de la Monte SM. Ethanol inhibition of insulin signaling in hepatocellular carcinoma cells. Alcohol Clin Exp Res 1998;22:2093–101.
[7] Zhang FX, Rubin R, Rooney TA. Ethanol induces apoptosis in cerebellar granule neurons by inhibiting insulin-like growth factor 1 signaling. J Neurochem 1998;71:196–204.
[8] Bhave SV, Ghoda L, Hoffman PL. Brain-derived neurotrophic factor mediates the anti-apoptotic effect of NMDA in cerebellar granule neurons: signal transduction cascades and site of ethanol action. J Neurosci 1999;19:3277–86.
[9] de la Monte SM, Ganju N, Tanaka S, Banerjee K, Karl PJ, Brown NV, et al. Differential effects of ethanol on insulin-signaling through the insulin receptor substrate-1. Alcohol Clin Exp Res 1999;23:770–7.
[10] Seiler AE, Ross BN, Green JS, Rubin R. Differential effects of ethanol on insulin-like growth factor-I receptor signaling. Alcohol Clin Exp Res 2000;24:140–8.
[11] Seiler AE, Ross BN, Rubin R. Inhibition of insulin-like growth factor-1 receptor and IRS-2 signaling by ethanol in SH-SY5Y neuroblastoma cells. J Neurochem 2001;76:573–81.
[12] Hallak H, Seiler AE, Green JS, Henderson A, Ross BN, Rubin R. Inhibition of insulin-like growth factor-I signaling by ethanol in neuronal cells. Alcohol Clin Exp Res 2001;25:1058–64.
[13] Resnicoff M, Sell C, Ambrose D, Baserga R, Rubin R. Ethanol inhibits the autophosphorylation of the insulin-like growth factor 1 (IGF-1) receptor and IGF-1-mediated proliferation of 3T3 cells. J Biol Chem 1993;268:21777–82.
[14] Resnicoff M, Rubini M, Baserga R, Rubin R. Ethanol inhibits insulin-like growth factor-1-mediated signalling and proliferation of C6 rat glioblastoma cells. Lab Invest 1994;71:657–62.
[15] Luo J, Miller MW. Platelet-derived growth factor-mediated signal transduction underlying astrocyte proliferation: site of ethanol action. J Neurosci 1999;19:10014–25.
[16] Ghiselli G, Chen J, Kaou M, Hallak H, Rubin R. Ethanol inhibits fibroblast growth factor-induced proliferation of aortic smooth muscle cells. Arterioscler Thromb Vasc Biol 2003;23:1808–13.
[17] Ullrich A, Gray A, Tam AW, Yang-Feng T, Tsubokawa M, Collins C, et al. Insulin-like growth factor I receptor primary structure: comparison with insulin receptor suggests structural determinants that define functional specificity. EMBO J 1986;5:2503–12.
[18] Werner H, Adamo M, Roberts Jr CT, LeRoith D. Molecular and cellular aspects of insulin-like growth factor action. Vitam Horm 1994;48:1–58.
[19] Seiler AE, Henderson A, Rubin R. Ethanol inhibits insulin receptor tyrosine kinase. Alcohol Clin Exp Res 2000;24:1869–72.
[20] Hubbard SR, Wei L, Ellis L, Hendrickson WA. Crystal structure of the tyrosine kinase domain of the human insulin receptor. Nature 1994;372:746–54.
[21] Favelyukis S, Till JH, Hubbard SR, Miller WT. Structure and autoregulation of the insulin-like growth factor 1 receptor kinase. Nat Struct Biol 2001;8:1058–63.
[22] Munshi S, Kornienko M, Hall DL, Reid JC, Waxman L, Stirdivant SM, et al. Crystal structure of the Apo, unactivated insulin-like growth factor-1 receptor kinase. Implication for inhibitor specificity. J Biol Chem 2002;277:38797–802.
[23] Wei L, Hubbard SR, Hendrickson WA, Ellis L. Expression, characterization, and crystallization of the catalytic core of the human insulin receptor protein-tyrosine kinase domain. J Biol Chem 1995;270:8122–30.
[24] Pautsch A, Zoephel A, Ahorn H, Spevak W, Hauptmann R, Nar H. Crystal structure of bisphosphorylated IGF-1 receptor kinase: insight into domain movements upon kinase activation. Structure 2001;9:955–65.

[25] Hubbard SR, Till JH. Protein tyrosine kinase structure and function. Annu Rev Biochem 2000;69:373–98.
[26] Lopaczynski W, Terry C, Nissley P. Autophosphorylation of the insulin-like growth factor I receptor cytoplasmic domain. Biochem Biophys Res Commun 2000;279:955–60.
[27] Zhang FX, Rubin R, Rooney TA. *N*-methyl-D-aspartate inhibits apoptosis through activation of phosphatidylinositol 3-kinase in cerebellar granule neurons. A role for insulin receptor substrate-1 in the neurotrophic action of *N*-methyl-D-aspartate and its inhibition by ethanol. J Biol Chem 1998;273:26596–602.
[28] Harrison RW, Weber IT. Molecular dynamics simulations of HIV-1 protease with peptide substrate. Protein Eng 1994;7:1353–63.
[29] Harrison RW, Kourinov IV, Andrews LC. The Fourier–Green's function and the rapid evaluation of molecular potentials. Protein Eng 1994;7:359–69.
[30] Harrison RW, Reed CC, Weber IT. Analysis of comparative modeling predictions for CASP2 targets 1, 3, 9, and 17. Proteins 1997;1(Suppl): 68–73.
[31] Weber IT. Molecular mechanics calculations on protein–ligand complexes. Dordrecht, The Netherlands: Kluwer Academic Publishers; 1998.
[32] Dwyer DS, Bradley RJ. Chemical properties of alcohols and their protein binding sites. Cell Mol Life Sci 2000;57:265–75.
[33] Xu B, Bird VG, Miller WT. Substrate specificities of the insulin and insulin-like growth factor 1 receptor tyrosine kinase catalytic domains. J Biol Chem 1995;270:29825–30.
[34] Meyer H. On the theory of alcohol narcosis. What property of anesthetics produces their anesthetic action? Arch Exper Path U Naunyn-Schmiedeberg 1899;42:109–18.
[35] Franks NP, Jenkins A, Conti E, Lieb WR, Brick P. Structural basis for the inhibition of firefly luciferase by a general anesthetic. Biophys J 1998;75:2205–11.
[36] Franks NP, Lieb WR. Molecular and cellular mechanisms of general anaesthesia. Nature 1994;367:607–14.
[37] Stubbs CD, Slater SJ. Ethanol and protein kinase C. Alcohol Clin Exp Res 1999;23:1552–60.
[38] Stubbs CD, Rubin R. Effect of ethanol on platelet phospholipase A2. Lipids 1992;27:255–60.
[39] Krasowski MD, Harrison NL. General anaesthetic actions on ligand-gated ion channels. Cell Mol Life Sci 1999;55:1278–303.
[40] Diamond I, Gordon AS. Cellular and molecular neuroscience of alcoholism. Physiol Rev 1997;77:1–20.
[41] Abraham MH, Lieb WR, Franks NP. Role of hydrogen bonding in general anesthesia. J Pharm Sci 1991;80:719–24.
[42] Eckenhoff RG, Johansson JS. Molecular interactions between inhaled anesthetics and proteins. Pharmacol Rev 1997;49:343–67.
[43] Wood SC, Tonner PH, de Armendi AJ, Bugge B, Miller KW. Channel inhibition by alkanols occurs at a binding site on the nicotinic acetylcholine receptor. Mol Pharmacol 1995;47:121–30.
[44] Wick MJ, Mihic SJ, Ueno S, Mascia MP, Trudell JR, Brozowski SJ, et al. Mutations of gamma-aminobutyric acid and glycine receptors change alcohol cutoff: evidence for an alcohol receptor? Proc Natl Acad Sci USA 1998;95:6504–9.
[45] Scheller M, Forman SA. Butanol effects on gamma-amino butyric acid concentration-responses in human alpha1beta2gamma2L gamma-amino butyric acid type A receptors with a mutation at alpha1S270. Neurosci Lett 2001;297:179–82.
[46] Forman SA, Zhou Q. Nicotinic receptor pore mutations create a sensitive inhibitory site for ethanol. Alcohol Clin Exp Res 2000;24: 1363–8.
[47] Harris T, Shahidullah M, Ellingson JS, Covarrubias M. General anesthetic action at an internal protein site involving the S4–S5 cytoplasmic loop of a neuronal K(+) channel. J Biol Chem 2000;275:4928–36.
[48] Ye Q, Koltchine VV, Mihic SJ, Mascia MP, Wick MJ, Finn SE, et al. Enhancement of glycine receptor function by ethanol is inversely correlated with molecular volume at position alpha267. J Biol Chem 1998;273:3314–9.
[49] Wilkemeyer MF, Charness ME. Characterization of ethanol-sensitive and insensitive fibroblast cell lines expressing human L1. J Neurochem 1998;71:2382–91.
[50] Mohammadi M, McMahon G, Sun L, Tang C, Hirth P, Yeh BK, et al. Structures of the tyrosine kinase domain of fibroblast growth factor receptor in complex with inhibitors. Science 1997;276:955–60.
[51] Gotoh N, Tojo A, Hino M, Yazaki Y, Shibuya M. A highly conserved tyrosine residue at codon 845 within the kinase domain is not required for the transforming activity of human epidermal growth factor receptor. Biochem Biophys Res Comm 1992;186:768–74.
[52] Xu J, Yeon JE, Chang H, Tison G, Chen GJ, Wands J, et al. Ethanol impairs insulin-stimulated neuronal survival in the developing brain: role of PTEN phosphatase. J Biol Chem 2003;278:26929–37.
[53] Weber IT. Molecular mechanics calculations on Rous sarcoma virus protease with peptide substrates. In: Harrison RW, editor. Protein Sci. 1997;6:2365–74.
[54] Mahalingam B, Cuesta-Munoz A, Davis EA, Matschinsky FM, Harrison RW, Weber IT. Structural model of human glucokinase in complex with glucose and ATP: implications for the mutants that cause hypo- and hyperglycemia. Diabetes 1999;48:1698–705.